

Journal Pre-proofs

Research paper

Hierarchical TiO₂ Microsphere Assembled from Nanosheets with High Photocatalytic Activity and Stability

Jie Hu, Yi Lu, Xiao-Fang Zhao, Yu-Qian Tang, Yuan-Zhou Li, Yu-Xuan Xiao, Zhi-Yi Hu, Bao-Lian Su, Xiao-Yu Yang

PII: S0009-2614(19)30970-4
DOI: <https://doi.org/10.1016/j.cplett.2019.136989>
Reference: CPLETT 136989

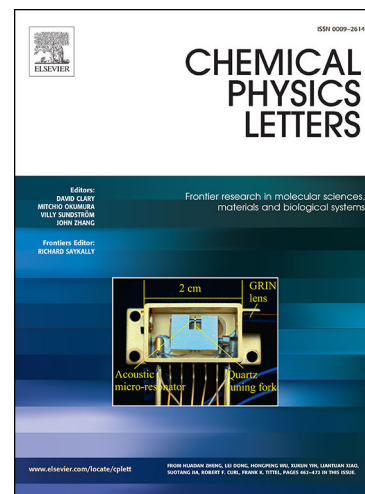
To appear in: *Chemical Physics Letters*

Received Date: 3 September 2019
Revised Date: 31 October 2019
Accepted Date: 25 November 2019

Please cite this article as: J. Hu, Y. Lu, X-F. Zhao, Y-Q. Tang, Y-Z. Li, Y-X. Xiao, Z-Y. Hu, B-L. Su, X-Y. Yang, Hierarchical TiO₂ Microsphere Assembled from Nanosheets with High Photocatalytic Activity and Stability, *Chemical Physics Letters* (2019), doi: <https://doi.org/10.1016/j.cplett.2019.136989>

This is a PDF file of an article that has undergone enhancements after acceptance, such as the addition of a cover page and metadata, and formatting for readability, but it is not yet the definitive version of record. This version will undergo additional copyediting, typesetting and review before it is published in its final form, but we are providing this version to give early visibility of the article. Please note that, during the production process, errors may be discovered which could affect the content, and all legal disclaimers that apply to the journal pertain.

© 2019 Published by Elsevier B.V.



Hierarchical TiO₂ Microsphere Assembled from Nanosheets with High Photocatalytic Activity and Stability

Jie Hu,^{§, a} Yi Lu,^{§, a} Xiao-Fang Zhao,^a Yu-Qian Tang,^b Yuan-Zhou Li,^a Yu-Xuan Xiao,^a Zhi-Yi Hu,^{*a, c} Bao-Lian Su^{*a, d} and Xiao-Yu Yang,^{*a, e}

[§] These authors contributed equally to this work.

^a State Key Laboratory of Advanced Technology for Materials Synthesis and Processing & School of materials science and engineering, Wuhan University of Technology, 122, Luoshi Road, Wuhan, 430070, China.

E-mail: xyyang@whut.edu.cn, baoliansu@whut.edu.cn.

^b School of Chemical Engineering, Northeast Electric Power University, 169, Changchun Road, Jilin, 132012, China.

^c Nanostructure Research Centre (NRC), Wuhan University of Technology, 122, Luoshi Road, Wuhan, 430070, China.

Email: zhiyi.hu@whut.edu.cn.

^d Laboratory of Inorganic Materials Chemistry (CMI), University of Namur, 61, rue de Bruxelles, B-5000 Namur, Belgium. E-mail: bao-lian.su@unamur.be.

^e School of Engineering and Applied Sciences, Harvard University, Cambridge, Massachusetts 02138, USA. E-mail: xyyang@seas.harvard.edu.

Graphical abstract

Highlights

- Ti-based hierarchical microsphere assembled from nanosheets was prepared.
- TM-S exhibited excellent catalytic activities of H₂ production.
- TM-S achieved photo-assisted benzyl alcohol selective oxidized to benzaldehyde.

- Surface F and nanosheets structure were suggested to explain enhanced performance.

Abstract

TiO₂ hierarchical microsphere assembled from anatase TiO₂ nanosheets has been successfully prepared and exhibited excellent catalytic activities of H₂ production and benzyl alcohol selective oxidized to benzaldehyde. These enhanced photoactivity can be mainly ascribed to the charge separation promoted by the surface F and nanosheet units, enhancement of substrate molecular transport profited from the hierarchical structure.

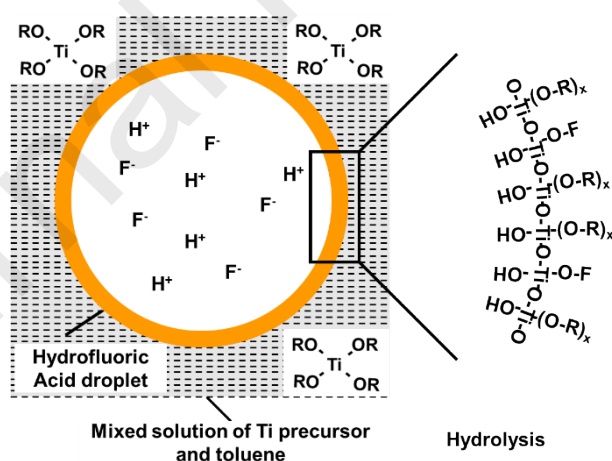
Keywords: TiO₂, hierarchical structure, nanosheet, photocatalysis

1. Introduction

Titania(TiO₂) is one of the most important semiconductors for advanced energy conversion and storage applications.^[1-3] Previous reports have demonstrated that catalytic activity and selectivity of TiO₂ materials are strongly dependent on their nano-architecture.^[4, 5] To date, nanosheets are emerging as a class of key materials in energy and environmental fields due to their atomic/electronic structures and intrinsic properties.^[6] These nanosheet materials in particular have large specific surface area and nano-scaled thickness, which not only offer the more reaction sites for catalytic reaction, but also prolong the separation of photoexcited carriers by the minimized transfer pathway.^[7, 8] Hierarchical functional structures have attracted great interest in recent years to enhance the structure stability and photoactivity through the oriented assembly of nanosized units or their aggregates.^[9, 10] Pre-formed nanosheets can be integrated with a three-dimensional (3D) material as a new building block to fabricate

interfacial heterostructures.^[11] However, it is still a big challenge to design and synthesize a perfect hierarchical functional structure with enhanced photocatalytic performances.

Herein, we report a template-free approach to synthesize TiO_2 hierarchical microspheres assembled from anatase TiO_2 nanosheets with activated $\{001\}$ facets. As shown in Scheme 1, nanosheets will grow within the microemulsion droplets and develop into a microsphere with a mixed phase of anatase TiO_2 and TiOF_2 (TM) under the presence of toluene. However, it has been reported by many researchers that TiOF_2 shows poor photocatalytic activity.^[12, 13] After heat treatment in air or solvothermal treatment in isopropyl alcohol,^[14, 15] TiOF_2 crystals can be converted into anatase TiO_2 with surface absorbed fluorine (F). The sample prepared with further solvothermal treatment exhibits highest photocatalytic activity on both hydrogen generation and selective oxidation of benzyl alcohol, which can be mainly ascribed as: (1) the charge separation promoted by the existence of surface fluorine (F) and nanosheets structure with exposed active facets, (2) enhancement of substrate molecular transport profited from the hierarchical structure.



Scheme 1. Schematic formation of Ti-based hierarchical microsphere (TM) assembled from nanosheets.

2 Experimental section

2.1. Materials

Hydrofluoric acid (SCRC, AR grade), toluene (SCRC, AR grade), titanium butoxide (TBT, Aladdin, 98.0%), benzyl alcohol (SCRC, 98%), commercial TiO₂ (anatase, 40 nm, SCRC) were used as purchased. All other chemicals were of AR grade and used as purchased.

Caution! Hydrofluoric acid is extremely corrosive and should be handled very carefully.

2.2. Synthesis of TM, TM-S, TM-C and TM-S-A

Ti-based microspheres (TM) constructed of nanosheets were synthesized through a solvothermal approach in a toluene-HF mixed solution using TBT as titanium source. The sample consists of anatase TiO₂ and TiOF₂. Typically, HF (40 wt %, 1.0 mL) was drop wised into a mixture solution of TBT (12.5 g) and toluene (2.0 mL) under vigorous stirring. And then, the reaction mixture was heated to 200 °C for 24 h. The light blue products were collected through membrane filtering (pore size, 0.45 μm) and washed with ethanol.

Sample named TM-S was prepared by solvothermal treatment of sample TM in suitable isopropyl alcohol (TBA) at 200°C for 24 h. Followed by washing TM-S powders with NaOH (0.1 M) and water several times, the control sample without surface F was prepared (denoted as TM-S-A). For the purpose of comparison, TiOF₂ crystals in TM also have been transformed into anatase TiO₂ by heat-treating of TM under 500°C in the air (denoted as TM-C).

2.3. Synthesis of TiO₂ (101) and TiOF₂

The {101}-exposed anatase TiO₂ and TiOF₂ were prepared by the route in the literature and denoted as TiO₂ (101)^[16] and TiOF₂^[15], respectively.

2.4. Characterization

The samples were characterized by X-ray diffraction (XRD, D8 ADVANCE, 40 kV, 40 mA) patterns with Cu Kα radiation (λ=1.54056 Å). The morphology, element distribution and structure were performed on a field-emission gun scanning electron

microscope (SEM, Hitachi S-4800, operated at 5 kV) and scanning/transmission electron microscope (S/TEM, Thermo Fisher Scientific Talos-F200S, fitted with Super-X EDS system, operated at 200 kV). The nitrogen adsorption-desorption isotherms were performed on a Micrometrics (TriStar II 3020 system, 77 K) after the samples were degassed at 120 °C for 12 h. Raman spectra were characterized by an Invia Raman Microscope (Invia Microscope, Renishaw, UK, 632.8 nm) at room temperature. The surface electronic states of F were obtained by X-ray photoelectron spectroscopy (XPS, VG Multilab 2000). The UV/vis spectroscopy diffuse reflectance spectra (UV/vis DRS) were performed on a UV/vis spectrophotometer (UV-2550). Time-resolved PL fluorescence spectra of samples suspended in aqueous solutions (pH 2.4) were characterized with a fluoromax-4 spectrofluorometer by excitation at 286 nm (HORIBA Scientific).

2.5. Evaluation of photocatalytic activity

2.5.1. Photocatalytic aerobic oxidation

Photocatalytic oxidation of benzyl alcohol was performed as follow: Firstly, the catalyst (16 mg) was added to the mixture solution of benzotrifluoride (1.5 mL), benzyl alcohol (0.1 mM) and dodecane (0.1 mM). The above reaction solution was transferred to a Pyrex glass bottle. And then, the solution was irradiated by a lamp (PLS-SXE 300C) under stirring. After being irradiated for 4h, the catalysts were removed through centrifugation and the remaining solution was analyzed by a gas chromatograph (GC-Agilent 7890A, FID). Conversion of benzyl alcohol and selectivity of benzaldehyde were calculated.

2.5.2 Photocatalytic hydrogen generation

Photocatalytic hydrogen generation was tested in a closed circulation system as follow: The catalyst (20 mg) was suspended in a mixture of deionized water (80 mL) and methanol (20 mL). Followed by adding a chloroplatinic acid aqueous solution (10 mM, 52 μ L), the reaction mixture was sealed in a quartz vessel and vacuumed. And then, the reaction mixture was irradiated by a lamp (PLS-SXE 300C) under stirring

and cooling. The generated H_2 was analyzed by gas chromatograph (GC-Agilent 7890A, TCD).

3. Results and discussion

The microstructure of as-prepared Ti-based microsphere (TM) was studied by scanning electron microscopy (SEM). It is apparent that the as-prepared microspheres with diameters about 5 μm are constructed of nanosheets with a length of 30-50 nm and a thickness of about 20 nm (Figure 1a). SEM images point out that the morphology of the sample was remained after solvothermal treatment (Figure S1a). However, the microsphere morphology of the material prepared was destroyed after alkali treatment, as exhibited in Figure S1b. And, calcination promotes the growth of crystallite and leads to the increasing of nanosheets' thickness and the gap between assembled nanosheets (Figure S1c, Table S1). As shown in Figure S1d, commercial TiO_2 is constructed by nanoparticles. The crystal compositions of the samples were confirmed by X-ray diffraction (XRD, Figure 1b). The diffraction peaks (at 23.4° and 25.3°) correspond to the (100) plane diffraction of cubic $TiOF_2$ (ICDD no. 00-08-0060) and the (101) plane diffraction of anatase TiO_2 (ICDD no. 01-0086-1157), respectively, which indicates that the TM is composed of mixed phases. The peak at 23.4° disappears after solvothermal treatment in TBA at 200°C for 24 h (Figure 1b red line), which suggests the beginning of $TiOF_2$ hydrolysis. It could be ascribed to the generation of a small amount of water during dehydration of isopropyl alcohol. Additionally, the XRD peak intensities of anatase phase in the TM-S sample become stronger and slightly narrower than the TM sample, indicating the enhanced crystallinity. The calcined sample (TM-C, Figure 1b brown line) also shows similar stronger intensities and narrower width of XRD diffraction peaks contributed to anatase phase. These experimental results indicate that cubic $TiOF_2$ phase can be transformed into anatase TiO_2 phase through calcination or solvothermal treatment. In addition, the crystal structure has no significant change after alkali

treatment (TM-S-A). The nitrogen adsorption-desorption isotherms were performed to confirm the porous structure and specific surface area of the samples (Figure 1c). These isotherm curves are type IV with type H3 hysteresis loop, indicating the existence of mesopores in aggregated nanosheets. This is consistent with the SEM image (Figure 1a). The specific surface areas of TM, TM-S, TM-S-A, TM-C, commercial TiO_2 were estimated to be 84, 82, 92, 57 and $7 \text{ m}^2\cdot\text{g}^{-1}$, respectively, which enables the different rate of diffusion in the solution and leads to the distinguished photocatalytic activity. From the pore size distribution data, the TM, TM-S, TM-S-A, TM-C show broad distribution of pore diameters centred at 22.7, 25.6, 15.7 and 36.9 nm, respectively (Figure S2 and Table S1). Corresponding to the isotherm curves, commercial TiO_2 does not show porous structure. Raman spectra (Figure 1d) were displayed to identify the well-crystallized structure of TM-S, TM-S-A, TM-C and commercial TiO_2 . The peaks ranging from 150 cm^{-1} to 700 cm^{-1} were attributed to the anatase crystallites of TiO_2 . Meanwhile, crystallites of TiOF_2 show no significant Raman peaks.

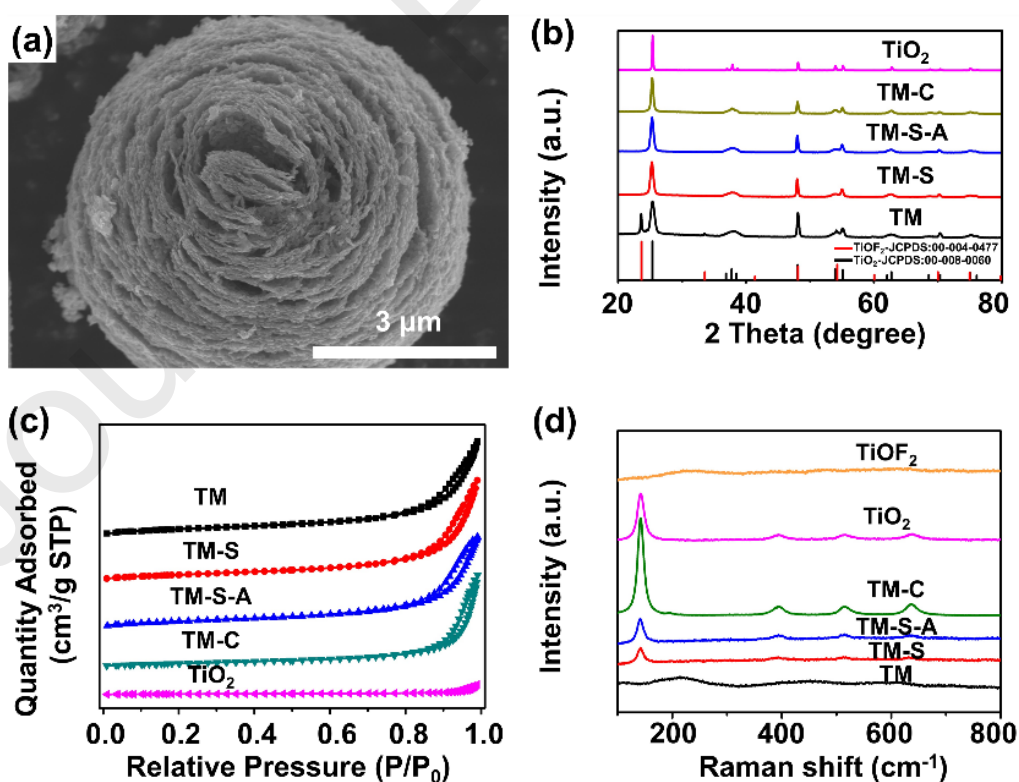


Figure 1. (a) SEM image of TM sample, (b) XRD patterns of TM, TM-S, TM-S-A, TM-C and commercial TiO₂, (c) Nitrogen adsorption-desorption isotherm curves of TM, TM-S, TM-S-A, TM-C, and commercial TiO₂, (d) Raman spectra of the TM, TM-S, TM-S-A, TM-C, commercial TiO₂ and TiOF₂.

The HAADF-STEM image (Figure 2a) and corresponding EDSElemental maps (Figure 2b-d) of TM-S sample show the nature of two-dimensional F-doping TiO₂ nanosheets. Corresponding to the XPS spectra (Figure S3), the element mapping image of F exhibits that surface F are uniformly distributed on the nanosheets. Surface F ions exhibit strong holes capture ability, which can reduce the recombination of electron-hole pairs and improve the photoactivity.^[17] The high resolution HAADF-STEM image (Figure 2e) and corresponding FFT (Figure 2e inset) reveal that the side surface of nanosheet is perpendicular to TiO₂ [100] zone axis and the {001} facet is the maximum exposed surface. Further, the atomic resolution HAADF-STEM image (Figure 2f) demonstrates the clean surface with different TiO₂ crystal facets, as the model is shown (Figure 2f inset). The TM-C sample has a similar structure composed of smaller and thicker TiO₂

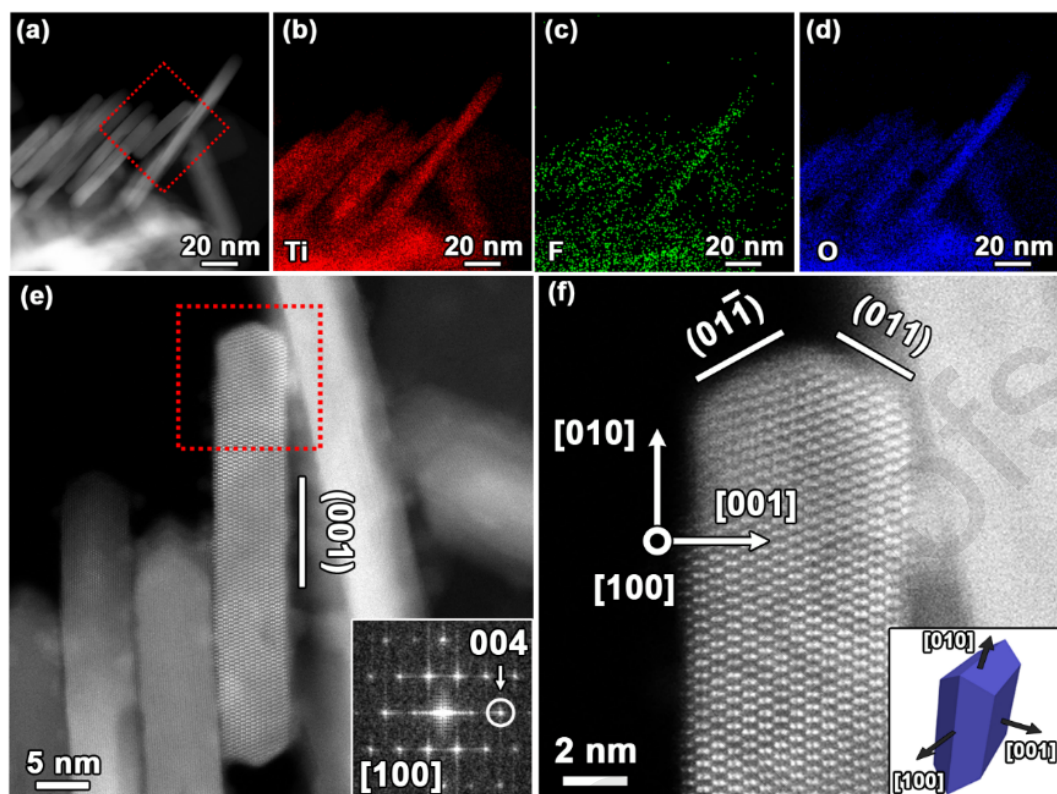


Figure 2. (a) HAADF-STEM image of TM-S sample, (b-d) corresponding EDS elemental maps: Ti (red), F (green), and O (blue), (e) HR-HAADF-STEM image of the area indicated by red box in (a) and corresponding FFT pattern (inset), (f) enlarged atomic resolution HAADF-STEM image of the area indicated by red box in (e) and corresponding model of TiO_2 nanoparticle (inset).

nanosheets but without surface F, making it possible to distinguish the effect of surface F ions without the disturbing of structure (Figure S4).

The photocatalytic activities of the samples were investigated through selective photo-assisted oxidation of benzyl alcohol to benzaldehyde, which is a common chemical reaction and very important for laboratory and commercial processes.^[18-20] Performances of the TM, TM-S, TM-S-A, TM-C, commercial TiO_2 under light irradiation and dark are presented in Figure 3a and Table S2. All of these samples show the selectivity of more than 99% for the photocatalytic oxidation of benzyl alcohol under irradiation and trace of photocatalytic activity under dark. TM and TM-S display obviously higher photoactivity (42.5% and 44.9%, respectively)

compared to TM-C (25.7%). The enhanced activity could be due to the existence of surface Ti-F groups, which exhibits strong electron capture ability and could reduce the recombination of electron-hole pairs and improve the photoactivity. It is further proved by the fact that TM-S-A and TM-S-2nd being free of F show similar conversion rate (23.0% and 23.5% respectively) to TM-C. H₂ generation from a water/methanol mixture solution (Figure 3b-c) and the change of the fluorescence intensity of terephthalic acid with irradiation time have been performed (Figure S5). TM-S (Figure 3b-c) not only shows the highest hydrogen production rate of 45 mmol·h⁻¹·g⁻¹, but also exhibits high stability after 5 cycles. STEM images exhibit that Pt nanoparticles are uniformly loaded onto the surface of TM-S and TM-C (Figure S6), indicating the performance difference is independent of Pt deposited. Corresponding to the results on the selective oxidation of benzyl alcohol to benzaldehyde, the surface F and hierarchal structure of TM-S benefit the enhanced photoactivity. To further confirm the beneficial effects of the surface F and hierarchical structure on the photocatalytic activity and chemistry of the samples, photoactivity (Figure S7), PL analysis (Figure S8a) and photocurrent density of samples were studied (Figure S8b). According to the XPS valence band and band gap calculated (Figure S7), sample TM-S, TM-S-A, TM-C and commercial TiO₂ show similar band structure, indicating the different photoactivity is irrelevant with band structure in this work. As shown in Figure S8a, the TM-S exhibits the lowest fluorescence intensity with excitation wavelength of 320 nm. The photocurrent density of TM, TM-S, TM-S-A and TiO₂ under UV/vis light irradiation were carried out. As shown in Figure S8b, TM-S shows the highest photocurrent intensity during these samples, indicating the most efficient charge separation and transfer. After treating by NaOH, the photocurrent of TM-S-A decreased, which mainly caused by the remove of surface F ions. Time-resolved PL decays of the TM, TM-S, TM-S-A, TM-C and commercial TiO₂ were performed to further compare the efficiency of charge separation (Figure S9). Due to the prolonged lifetime of photogenerated

carriers, the samples with efficient charge separation will show a slow PL signal decay.^[2, 22] As we can see in Figure S9 and the corresponding fitting and calculating results in Table S3, TM-S shows the longest photoluminescence lifetime (3.66 ns) because of the high efficiency in electron-hole separation benefited from surface F ions.^[23]

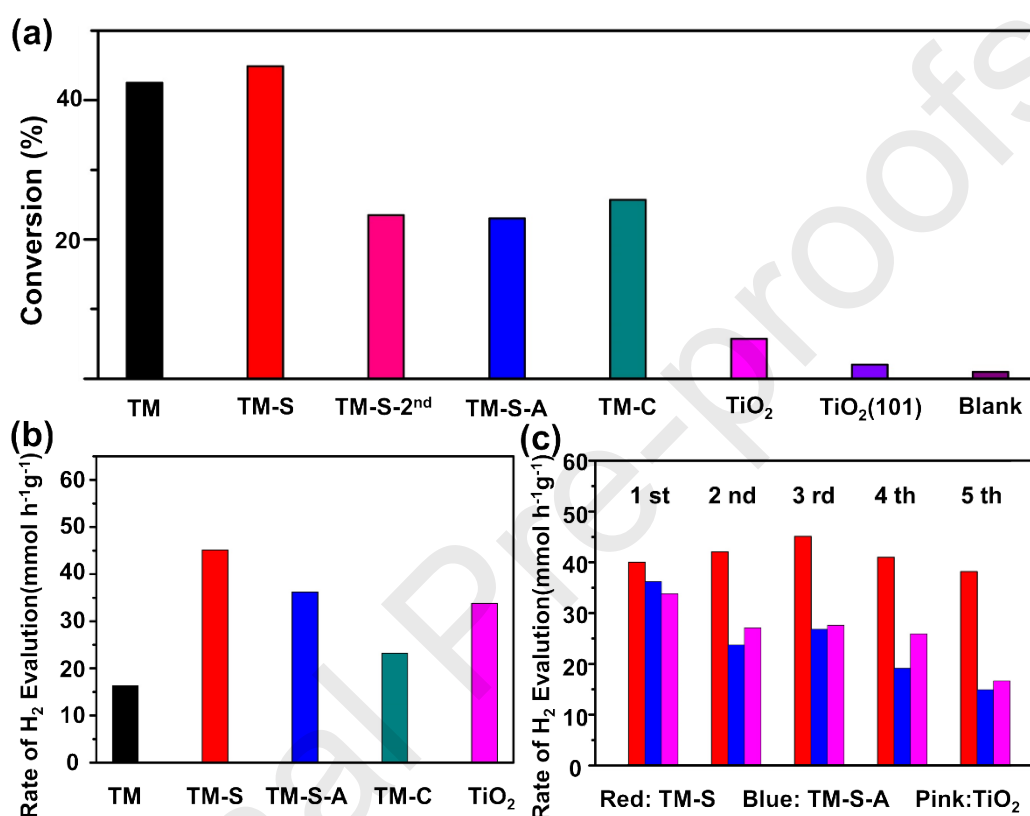


Figure 3. (a) Photocatalytic selective oxidation conversion of benzyl alcohol to benzaldehyde over TM, TM-S, TM-S-2nd, TM-S-A, TM-C, commercial TiO₂, TiO₂ (101) and blank,^a ^[21] (b) comparison of the photogeneration of H₂ from methanol aqueous solution after loading 0.5 wt% Pt on TM, TM-S, TM-S-A, TM-C and commercial TiO₂ under UV/vis light irradiation, and (c) cycle performance of the photogeneration of H₂ from methanol aqueous solution after loading 0.5 wt% Pt on TM-S, TM-S-A and commercial TiO₂ under UV/vis light irradiation. ^aReaction conditions: 1.5 mL of BTF; 0.1 mmol of benzyl alcohol; 0.1 mmol dodecane; 16 mg of catalysts; reaction for 4 h at room temperature.

The proposed reaction mechanism is briefly shown in Figure 4. According to the DFT calculations, Yu et al. pointed out that the {101} and {001} facets of anatase TiO₂ within a single crystal can form a surface heterojunction for they show different band edge positions.^[24] Under light irradiation, the photogenerated holes (h⁺) tend to move to {001} facets as oxidative sites, while photogenerated electrons are inclined to move to {101} facets as reductive sites.^[25] Moreover, the abundant surface undercoordinated Ti atoms and active oxygen atoms lead to the high reactivity of anatase {001}, which is provided by first-principles calculations.^[26-27] Thus the {001} facets become more active than {101} facets in photo-assisted oxidation reactions. In our case, the surface F anions with negative electric will attract the h⁺ to migrate to the surface of TiO₂ and inhibit the migration of photogenerated electrons,^[28] which further prevents electron-hole recombination. During the photocatalytic oxidation of benzyl alcohol, the O₂ adsorbed at defect sites will bond with photoelectrons and produce O₂⁻. These O₂⁻ can cleave the O-H bond of the alcohol and then evolve into an alkoxide intermediate which will combine with a proton from the reaction between h⁺ and H₂O to produce H₂O₂ and yield benzaldehyde.^[29] The nanosheet structure and surface F ions mainly contribute to the enhanced photoactivity of TM-S.

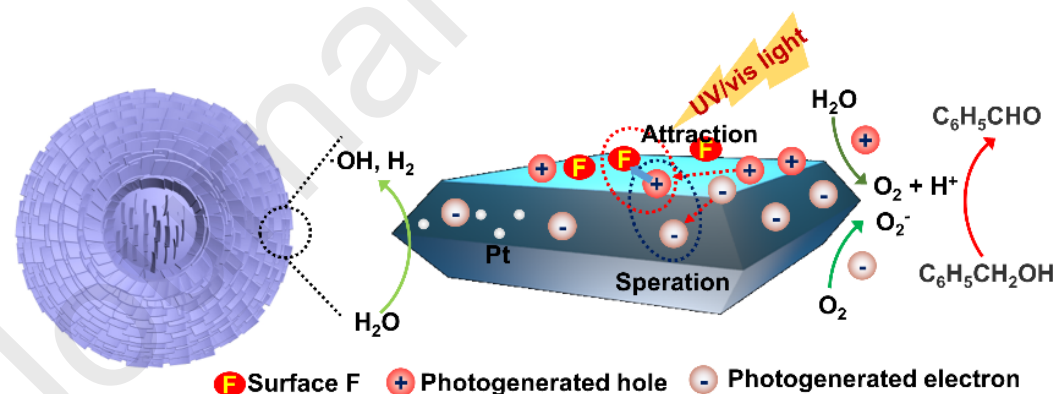


Figure 4. Proposed mechanism for the photocatalytic properties of TM-S.

4. Conclusions

In summary, we presented a synthetic strategy toward TiO₂ hierarchical microspheres assembled from anatase TiO₂ nanosheets. Through the evaluation of photocatalytic performance, these TiO₂ nanosheet spheres manifest a nearly twice of conversion efficiency (44.9%) in benzyl alcohol selective oxidized to benzaldehyde than counterpart (TM-S-A), relatively high ability of photocatalytic hydrogen generation (45 mmol·h⁻¹·g⁻¹) and high stability. The improved photocatalytic ability can be mainly attributed to the charge separation promoted by the existence of surface F and exposed {001} high-energy facets, enhancement of substrate molecular transport profited from the hierarchical structure.

Declaration of Competing Interest

The authors declare that they have no known competing financial interests or personal relationships that could have appeared to influence the work reported in this paper.

Acknowledgments

This work supported by National Key R&D Program of China (2017YFC1103800), PCSIRT (IRT_15R52), NSFC (U1663225, U1662134, 21711530705, 51503166, 51861135313), ISTCP (2015DFE52870), HPNSF (2016CFA033), the Fundamental Research Funds for Central Universities (WUT:2019III012GX), Jilin Province Science and Technology Development Plan (20180101208JC). The authors thank the National Center for Magnetic Resonance in Wuhan for Time-resolved PL.

References

- [1] J. Nowotny, M. A. Alim, T. Bak, M. A. Idris, M. Ionescu, K. Prince, M. Z. Sahdan, K. Sopian, M. A. M. Teridie, W. Sigmundf, *Chem. Soc. Rev.* 44 (2015) 8424-8442.

- [2] Y. Lu, X. Cheng, G. Tian, H. Zhao, L. He, J. Hu, S.-M. Wu, Y. Dong, G.-G. Chang, S. Lenaerts, S. Siffert, G. Van Tendeloo, Z.-F. Li, L.-L. Xu, X.-Y. Yang, B.-L. Su, *Nano Energy* 47 (2018) 8-17.
- [3] J. Hu, T. Zhao, W. Geng, Y. Lu, X. Zhao, Y. Li, Y. Tang, J. Liu, L. Wang, C. Janiak, X. Yang, B. Su, *Chem. Commun.* 55 (2019) 9275-9278.
- [4] J. Tian, Z. Zhao, A. Kumar, R. I. Boughton, H. Liu, *Chem. Soc. Rev.* 43 (2014) 6920-6937.
- [5] S. M. Wu, X. L. Liu, X. L. Lian, G. T., C. Janiak, Y. X. Zhang, Y. Lu, H. Z. Yu, J. Hu, H. Wei, H. Zhao, G. G. Chang, G. V. Tendeloo, L. Y. Wang, X. Y. Yang, B. L. Su, *Adv. Mater.* 30 (2018) 1802173.
- [6] C. Tan and H. Zhang, *Chem. Soc. Rev.* 44, (2015) 2713-2731.
- [7] Y. Dong, S. Y. Chen, Y. Lu, Y. X. Xiao, J. Hu, S. M. Wu, Z. Deng, G. Tian, G. G. Chang, J. Li, S. Lenaerts, C. Janiak, X. Y. Yang, B. L. Su, *Chem.-Asian J.* 13 (2018) 1609-1615.
- [8] M. Faraji, M. Yousefi, S. Yousefzadeh, M. Zirak, N. Naseri, T. H. Jeon, W. Choi and A. Z. Moshfegh, *Energy Environ. Sci.* 12 (2019) 59-95.
- [9] X.-Y. Yang, L.-H. Chen, Y. Li, J. C. Rooke, C. Sanchez and B.-L. Su, 46 (2017) 481-558.
- [10] Z.-C. Wu, Y. Lu, Y. Wang, Y.-Z. Li, L. He, X. Cheng, W. Geng, J. Ying, G.-G. Chang, *Chem. Phys. Lett.* 708 (2018) 32-36.
- [11] S. Liu, J. Yu, M. Jaroniec, *Chem. Mater.* 23 (2011) 4085-4093.
- [12] Z. Wang, K. Lv, G. Wang, K. Deng, D. Tang. *Appl. Catal. B* 100 (2010) 378-385.
- [13] K. Lv, J. Yu, L. Cui, S. Chen, M. Li, *J. Alloys Compd.* 509 (2011) 4557-4562.
- [14] C. Z. Wen, Q. H. Hu, Y. N. Guo, X. Q. Gong, S. Z. Qiao and H. G. Yang, *Chem. Commun.* 47 (2011) 6138-6140.
- [15] Z. Huang, Z. Wang, K. L. Lv, Y. Zheng, K. Deng, *ACS Appl. Mater. Interfaces* 5 (2013) 8663-8669.

- [16] M.-H. Yang, P.-C. Chen, M.-C. Tsai, T.-T. Chen, I.-C. Chang, H.-T. Chiu and C.-Y. Lee, *CrystEngComm* 15 (2013) 2966-2971.
- [17] M. Chen, J. Ma, B. Zhang, G. He, Y. Lia, C. Zhang and H. He, *Appl. Catal. B* 207 (2017) 397-403.
- [18] M. Fujihira, Y. Satoh and T. Osa, *Nature* 293 (1981) 206-208.
- [19] J. C. Colmenares, W. Ouyang, M. Ojeda, E. Kuna, O. Chernyayeva, D. Lisovytskiy, S. De, R. Luque, A. M. Balu, *Appl. Catal. B* 183 (2016) 107-112.
- [20] L. Chen, J. Tang, L.-N. Song, P. Chen, J. He, C.-T. Au, S.-F. Yin, *Appl. Catal. B* 242 (2019) 379-388.
- [21] L. Shen, M. Luo, L. Huang, P. Feng and L. Wu, *Inorg. Chem.* 54 (2015) 1191-1193.
- [22] K. Fujihara, S. Izumi, T. Ohno, M. Matsumura, *J. Photochem. Photobiol. A* 132 (2000) 99-104.
- [23] M. J. Ruedas-Rama, A. Orte, E. A. H. Hall, J. M. Alvarez-Peza and E. M. Talavera, *Analyst* 137 (2012) 1500-1508.
- [24] J. Yu, J. Low, W. Xiao, P. Zhou, and M. Jaroniec, *J. Am. Chem. Soc.* 136 (2014) 8839-8842.
- [25] M. D'Arienzo, J. Carbajo, A. Bahamonde, M. Crippa, S. Polizzi, R. Scotti, L. Wahba, F. Morazzoni, *J. Am. Chem. Soc.* 133 (2011) 17652-17661.
- [26] A. Vittadini, A. Selloni, F. P. Rotzinger, M. Grätzel, *Phys. Rev. Lett.* 81 (1998) 2954-2957.
- [27] A. Selloni, *Nat. Mater.* 7 (2008) 613-615.
- [28] H. Sheng, Q. Li, W. Ma, H. Ji, C. Chen, J. Zhao, *Appl. Catal. B* 138-139 (2013) 212-218.
- [29] Y. Chen, W. Li, J. Wang, Y. Gan, L. Liu, M. Ju, *Appl. Catal. B* 191 (2016) 94-105.